Russian Journal of General Chemistry, Vol. 72, No. 6, 2002, pp. 886–892. Translated from Zhurnal Obshchei Khimii, Vol. 72, No. 6, 2002, pp. 948–955.

Grignard Reaction as a Result of Tunneling of the Triplet Branch of the Reaction Through a Singlet Barrier

A. A. Tulub

Ukhtomskii Research Institute of Physiology, St. Petersburg State University, St. Petersburg, Russia

Received November 9, 2000

Abstract — Quantum-chemical calculations were carried out to study the mechanism of the Grignard reaction Mg + CH_3F. The reaction between Mg and CH_3F gives rise to a triplet complex which has a lower energy than the corresponding singlet complex at $MgFCH_3$ angles ranging from 60 to 139°. The transition from the singlet branch of the reaction to the nonequilibrium triplet branch results in decomposition of CH_3F with formation of various final products. A linear Grignard reagent CH_3–Mg–F is formed by simultaneous homolytic CH_3–F dissociation and ionic covalent interaction of the methyl group and the fluorine atom with the magnesium cation arising in the course of the reaction. Normal mode frequencies for the Mg + CH_3F complex at various $MgFCH_3$ are were calculated. The calculation results nicely agree with experimental data.

Despite the extensive use of Grignard reagents in organic synthesis [1, 2], the mechanism of formation of alkylmagnesium halides RMgX (Grignard reaction) is still highly disputable [3, 4]. The lack of clear notion of the way of formation of Grignard reagents, in its turn, makes the mechanism of reactions involving these reagents difficult to understand. Nowadays, RMgX formation (the reaction proceeds when metallic magnesium is added to an appropriate alkyl halide in dry ether or tetrahydrofuran) is most commonly explained in terms of Walborsky's hypothesis assuming a radical reaction mechanism [5, 6]. Metallic magnesium loses an electron to RX to form radical anion RX which then dissociates into $R^{\cdot}$ and X^-. Anion X^- reacts with Mg^+, forming magnesium halide $MgX^{\cdot}$. The latter combines with radical $R^{\cdot}$ to give the Grignard reagent. The last stage of the above mechanism seems to be the most vulnerable, since the fate of the unpaired electron still remains unclear. Another hypothesis which, too, belongs to Walborsky [7], suggests that the Grignard reaction proceeds via formation of two radicals, $R^{\cdot}$ and $MgX^{\cdot}$. Therewith, it is unclear how the unpaired electron emerges on magnesium halide. However, the most elusive aspect of both Walborsky's mechanisms is the reason why the radicals arise. Electron promotion from Mg to the unoccupied σ^* orbital of the C-X bond (initial stage) does not seem realistic in the absence of a strong excitation source, since the energy gap between the occupied and unoccupied orbitals is fairly large (>10 eV). Moreover, the evidence obtained in experiments on formation of Grignard reagents in a noble gas medium argues against radical formation [8].

Davis [9] suggested a nonradical mechanism to account for the Grignard reaction. The author carried out quantum-chemical calculations to show that magnesium atom is capable of insertion into the R–X bond via an intermediate state. However, the mechanism responsible for this process accompanied by R–X bond cleavage and Mg–C and Mg–X bond formation is not yet established. The most elusive is the formation of a great number of side products which can be detected experimentally [10, 11].

The problem whether the Grignard reaction proceeds by a radical or a nonradical mechanism still remains unresolved. Of particular interest is the recent work by Bare and Andrews [10] who proposed that laser irradiation of magnesium surface can produce transition of the metal to a triplet state. Reaction of $Mg(^3P)$ with RX results in formation of an excited molecule $[RMgX]^*$ whose inactivation gives rise to a variety of products identified by IR spectroscopy [10, 11]. It seems probable that laser irradiation of magnesium atoms induces a cascade of reactions. It will, however, be remembered that the classical Grignard reaction does not imply using high-energy pulse sources, but gives, according to recent IR spectral data, the same products.

In the present study a new, triplet–singlet, mechanism of the Grignard reaction is proposed on the basis of quantum-chemical calculations. The mechanism accounts for a number of questions linked to the reaction discovered by Grignard as early as 1900 [12, 13]. The obtained results mostly relate to the reaction Mg + $CH_3F \rightarrow CH_3MgF$. The use of other

1070-3632/02/7206-0886 $27.00 © 2002 MAIK "Nauka/Interperiodica"

methyl or ethyl halides does not affect significantly the interpretation of the mechanism. Moreover, the products of magnesium reaction with methyl fluoride have been most reliably identified [10].

CH_3F. To answer the question why the Grignard reaction is accompanied by Mg insertion between the methyl group and fluorine, one should understand the nature of H_3C–F bond cleavage. Methyl fluoride in its ground singlet (S) state is stable (Fig. 1, curve S). The enthalpy of formation of the molecule ΔH is –60.951 kcal/mol, and the C–F bond length r[C–F] is 1.365 Å; these values agree with published data [14]. Transition of CH_3F to the excited triplet (T) state (Franck–Condon transition with spin unpairing at r[C–F] 1.365 Å) renders it unstable. The molecule dissociates (Fig. 1, curve T), yielding CH_3 and F fragments, according to reactions (1) and (2):

$$[CH_3F]^S \longrightarrow [CH_3F]^T, \quad (1)$$

$$[CH_3F]^T \longrightarrow CH_3^{\cdot} + F^{\cdot}. \quad (2)$$

The total enthalpy of reactions (1) and (2) is 113.973 kcal/mol. While in the singlet state carbon bears a positive charge (q 0.261) and F, negative (q –0.246), excitation to the triplet state (r[C–F] 1.365 Å) produces charge inversion: q(C) –0.258 and q(F) 0.150 (Table 1). Upon complete breakdown of the molecule (according to the calculation, CH_3 and F influence each other up to r[C–F] 6 Å), both the methyl group and the fluorine atom become neutral [reaction (2), Table 1). Curve T (Fig. 1) corresponds to a covalent branch of the reaction. Curve S relates to forced dissociation of CH_3F, resulting in formation of the same products. At r[C–F] 6.52 Å (bifurcation point), curves T and S intersect. Beyond the bifurcation point, curve T passes below curve S. The energy gap is not significant: 0.13×10^{-3} kcal/mol. Actually, the singlet and triplet states are mixed at r[C– F] > 6.0 Å.

Reaction (2) corresponds to homolytic dissociation of the C–F bond into two doublet (s = 1/2) fragments: $CH_3^{\cdot}$ and $F^{\cdot}$. Figure 2 shows localization of spin densities in the two fragments (r[C–F] 6.52 Å). Probably, in solutions the fluorine atom passes into an anion [reaction (3)] with the concomitant decrease in the total energy of 36.024 kcal/mol (direct quantum-chemical calculations):

$$F^{\cdot} + \bar{e} \longrightarrow F^{-}. \quad (3)$$

The $CH_3^{\cdot}$ fragment is stable in the gas phase. However, in solution, under certain conditions (occurrence of an exothermic side process, e.g. Grignard reaction, etc.), it can either assume the cationic form CH_3^+ [reaction (4)] or dissociate into two fragments [reaction (5)] with the subsequent transition $H^{\cdot} \rightarrow H^+$ [reaction (6)].

Table 1. Main characteristics of the CH_3F molecule in the singlet (S) and triplet (T) states[a]

Atom	q	E_{tot}
	$[CH_3F]^S$, r[C–F] 1.365 Å	
C	0.261	–87247.226
F	–0.246	
H	0.005	
	$[CH_3F]^T$, r[C–F] 1.365 Å	
C	–0.257	–87037.477
F	0.150	
H	0.036	
	$[CH_3–F]^T$, r[C–F] 6.52 Å	
C	–0.090	–87107.448
F	0.000	
H	0.030	

[a] (q) Effective atomic charge and (E_{tot}) total energy, kcal/mol. The q(H) values are averaged over three hydrogen atoms.

$$CH_3^{\cdot} - \bar{e} \longrightarrow CH_3^+, \quad (4)$$

$$CH_3^{\cdot} \longrightarrow :CH_2 + H^{\cdot}, \quad (5)$$

$$H^{\cdot} - \bar{e} \longrightarrow H^+. \quad (6)$$

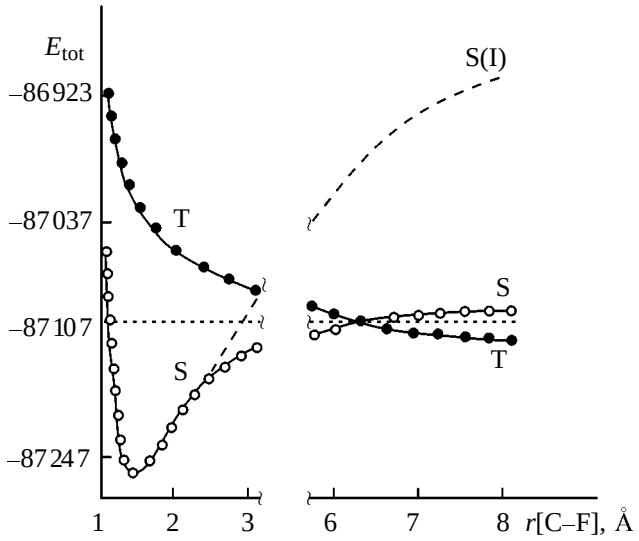

Fig. 1. Change of the total energy E_{tot} (kcal/mol) of the CH_3F molecule along the reaction coordinate r[C–F] for the singlet S (ground) and triplet T (excited) states. Curves S and T correspond to homolytic dissociation of CH_3F into two neutral doublet products $CH_3^{\cdot}$ and $F^{\cdot}$ (covalent branches). Curve S(I) relates to approach of the ionic forms CH_3^+ and F^- to each other to give CH_3F (ionic branch).

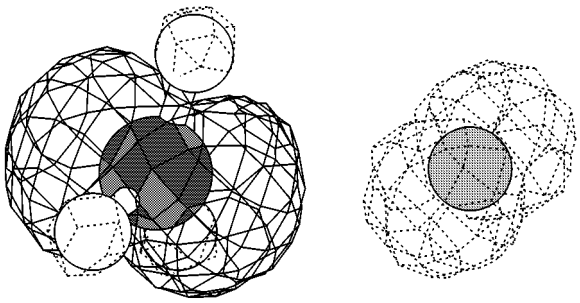

Fig. 2. Three-dimensional map of spin density for $CH^{\cdot}$ and $F^{\cdot}$, formed by dissociation of the CH_3F molecule, r[C–F] 6.52 Å.

Quantum-chemical calculations of the combined reaction (7) [reaction (2) and reaction (5)] show that the enthalpy of $:CH_2$, $H^{\cdot}$, and $F^{\cdot}$ formation from CH_3F is higher than the enthalpy of formation of the products of reaction (2) by 18.381 kcal/mol.

$$[CH_3F]^T \longrightarrow :CH_2 + H^{\cdot} + F^{\cdot}. \quad (7)$$

Reaction (7) reaches a plateau at r[C–F] ≥ 6.70 Å and r[C–H] ≥ 5.717 Å. In solution, the $H^{\cdot}$ and $F^{\cdot}$ radicals formed by reaction (7) assume the corresponding ionic forms [reactions (3) and (6)]. With account for solvation, reaction (8) may prove energetically favorable [15].

$$[CH_3F]^T \longrightarrow :CH_2 + HF. \quad (8)$$

Three major conclusions can be drawn on the basis of the calculation data for plausible conversions involving CH_3F. First, the chemistry of methyl fluoride in the triplet state is much more diversified than the chemistry of this compound in the singlet state. Decomposition of CH_3F can give rise to a number of different products. Second, in the absence of a source of high-energy excitation (laser, heating, etc.) capable of transferring CH_3F to the triplet state, reactions (2)–(8) are unlikely, since the energies of the triplet and singlet states (r[C–F] 1.365 Å) differ dramatically: $\Delta E(T–S)_{tot}$ 174.923 kcal/mol. That is why CH_3F shows no tendency for decomposition under normal conditions: Curve S (Fig. 1) corresponds to a deep minimum. Third, the curves of the singlet and triplet states can intersect (bifurcation point, Fig. 1). Besides the above-mentioned intersection of curves T and S at r[C–F] 6.52 A (this point is of minor interest, because decomposition products are the same for both branches), the singlet, S(I), branch (dashed line) and the triplet one intersect at r[C–F] 3.15 Å. Curve S(I) (Fig. 1) corresponds to the ionic reaction path generating the charged particles CH_3^+ and F^-. In the vicinity of the above-mentioned bifurcation point (rather hypothetical in terms of the principle of minimum energy reaction path (MERP) [16], the covalent (curve T) and ionic [curve S(I)] components can mix, which, in particular was observed in decompositions of ICN, NaI, and some other compounds [17–19].

Table 2. Calculated ν_{calc} and experimental ν_{exp} [10] frequencies (cm^{-1}) of normal modes for the CH_3F molecule

Group, bond[a]	ν_{calc} (I[b], km/mol)	ν_{exp}	
		solid argon	gas phase
C–F (str)	1042.8 (124.2)	1039.9	1048.2
C–H (str, s)	2955.6 (35)	2968.4	2864.5
C–H (str, as)	3139.8 (38)	3017.6	2982.2
Me (rock)	1195.8 (0.8)	1182.9	1195.5
Me (def, s)	1487.4 (2.3)	1462.4	1475.3
Me (def, as)	1496.2 (5)	1463.4	1471.1

[a] (str) Stretching modes, (def) deformation modes, (rock) rocking modes, (s) symmetric modes, and (as) asymmetric modes. [b] Intensity.

The calculated characteristics of the singlet and triplet states of the CH_3F molecule are given in Table 1, and the calculated frequencies and intensities of normal modes of CH_3F are shown in Table 2. The resulting data (Table 2) agree well with experimental frequencies [10] and those obtained by B3LYP calculations [20, 21].

Mg + CH_3F. The Grignard reaction is convenient to consider in terms of the Mg–F–C angle as reaction coordinate. Let this angle be zero, when the metal attaches to fluorine and forms one line with the F–C bond. Vice versa, if the metal inserts between F and C and lies on the straight line joining the three atoms, the angle is let be 180°.

The calculated total energies E_{tot} of the reaction Mg + CH_3F at varied MgFC angles (hereinafter, θ) for the singlet (S) and triplet (T) states are listed in Fig. 3. The total energy (branch S) slowly decreases at 0 ≤ θ ≤ 380. The instability of the state is due to the fact that magnesium bears a small negative charge [q(Mg) –0.075 to –0.001] in this θ range. By virtue of electrostatic repulsion, magnesium tends to leave the unfavorable zone of interaction with fluorine. At θ 44.20° (Table 3), the system reaches a local energy minimum [q(Mg) 0.042, q(F) –0.245, and q(C) 0.260]. The r[Mg–F] distance decreases from 2.201 Å

Table 3. Normal mode frequencies (ν, cm^{-1}), bond lengths (r, Å), atomic charges (q), and total energies (E_{tot}, kcal/mol) at five θ angles for the Grignard reaction (Fig. 3)

Parameter	θ 44.2° (S)	θ 67.8° (bif1)	θ 98.1° (TS)	θ 138.9° (bif2)	θ 180°
C–F (str)	1039.2 (124)	923.1 (12)	806.04 (0.7)	[a]	[a]
C–H (str, s)	2954.1 (35)	2949.2 (32)	2929.4 (23)	[a]	2912.8 (30)
C–H (str, as)	3129.2 (38)	3122.4 (33)	3096.6 (21)	[a]	3077.5 (17)
Me (rock)	1189.4 (0.8)	1142.3 (0.7)	984.2 (2.7)	659.2 (63)	615.4 (95)
Me (def, s)	1495.2 (2.4)	1482.1 (2.2)	1378.7 (1.3)	1214.8 (0.1)	1194.7 (0.01)
Me (def, as)	1507.3 (5)	1498.5 (4.7)	1491.1 (1.9)	1485.8 (0.4)	1481.5 (0.1)
Mg–F (str)	685.1 (0.2)	675.2 (0.1)	[a]	[a]	[a]
C–Mg–F (str, s)	[a]	[a]	[a]	423.5 (0.7)	469.7 (0.9)
C–Mg–F (str, as)	[a]	[a]	[a]	738.3 (73)	756.2 (108)
C–Mg–F (bend)[b]	[a]	[a]	[a]	129.5 (25)	134.2 (54)
r[Mg–F]	2.141	2.203	2.029	1.987	2.116
r[Mg–C]	3.262	2.996	2.584	2.218	1.979
r[C–F]	1.367	1.368	1.897	3.293	4.095
E_{tot}	–212384.123	–212374.745	–212347.973	–212420.128	–212454.149
q(Mg)	0.042	0.108	0.344	0.833	0.877
q(C)	0.260	0.196	–0.063	–0.578	–0.595
q(F)	–0.245	–0.268	–0.408	–0.634	–0.647

[a] The mode is lacking or not identified. [b] (bend) Bending modes.

(θ 5.80) to 2.141 Å (θ 44.20), while the other distance r[Mg–C] becomes equal to 3.262 Å. The local minimum can be assigned to the so-called van der Waals complex (CH_3F)–(Mg) (the term was introduced in [10]). Its distinguished feature is that both subsystems, CH_3F and Mg, remain unperturbed. The atomic charges and distances are practically the same as for the isolated molecules (Table 1). The normal mode frequencies differ insignificantly from those observed for the methyl group and C–F bond (Table 2). The Mg–F stretchings are of low intensity, which points to a weak magnesium– fluorine bonding. The angular structure as one of stable states of the Grignard reagent (at small θ angles) was earlier reported in [9].

Beyond the point of local minimum (θ 44.20°), curve S ascends and reaches a maximum at θ 98.10°, which corresponds to transition state TS (Table 3). The the point of maximum on the E_{tot} – θ curve corresponds to a potential barrier of 36.15 kcal/mol (Fig. 3). The latter value nicely fits (within 3 kcal/mol) that obtained by MP2/6-311G(d,p) calculations [9]. However, the interatomic distances are slightly different, especially the Mg–F length which is 0.146 Å shorter than that reported in [9]. The transition state is characterized by a high positive charge on the magnesium atom and a considerable negative charge on the fluorine atom. The Mg–C is shorter (r[Mg–C] 2.584 Å) than in the local minimum (θ 44.20°). However, it is still too long to be regarded as purely chemical. Evidence for the latter conclusion comes from the fact that the intensity of the Mg–C stretchings at ν 740 cm^{-1} (Table 3) is extremely low (0.07).

Beyond the point of maximum, curve S smoothly descends and reaches a minimum at θ 178.30°, which closely (within one degree) corresponds to a linear structure of the Grignard reagent CH_3–Mg–F. The calculated mode frequencies and intensities are

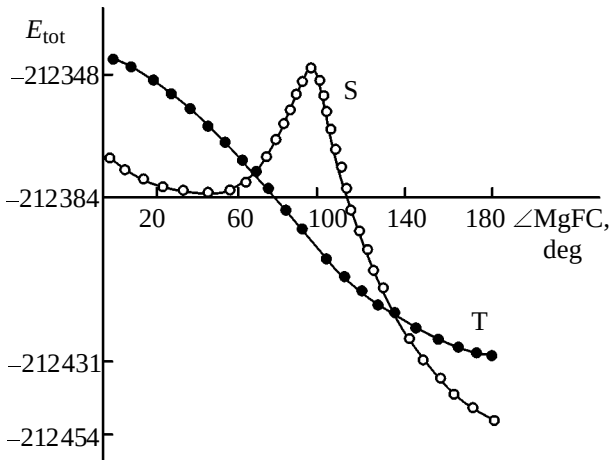

Fig. 3. Total energy E_{tot} (kcal/mol) of the Grignard reagent vs. MgFC angle (0 and 180° correspond to linear molecules Mg–F–CH_3 and F–Mg–CH_3, respectively).

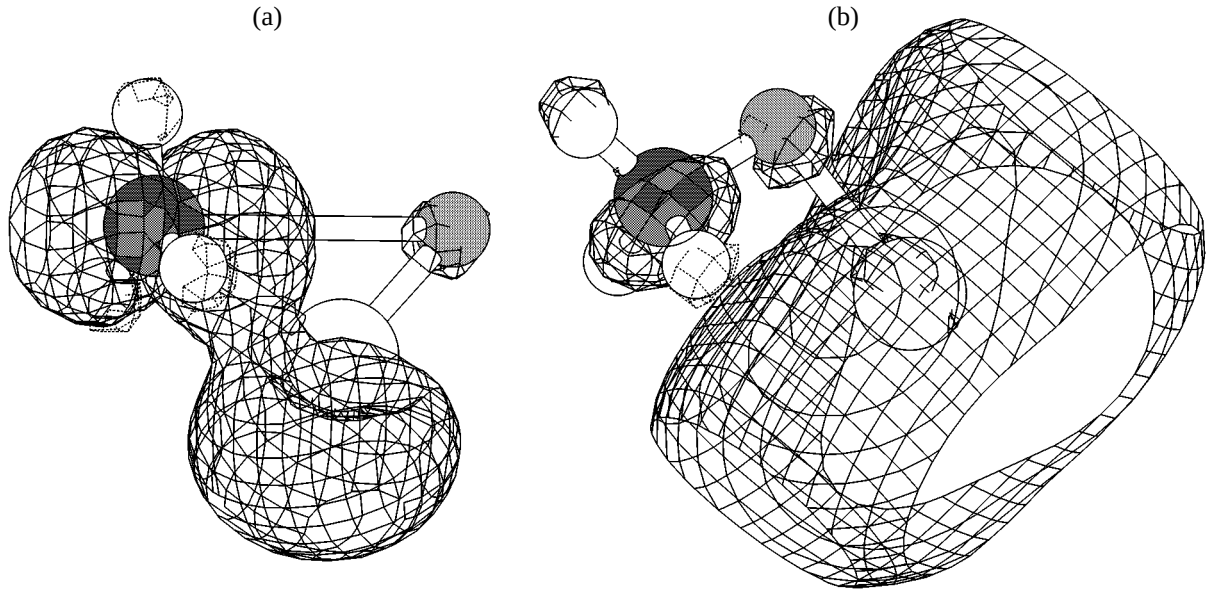

Fig. 4. Three-dimensional map of spin density for the Grignard complex CH_3–Mg–F. (a) θ 125.40°, *r*[C–F] 3.193 Å, *r*[Mg–C] 2.303 Å, *r*[Mg–F] 1.771 Å, *q*(Mg) 0.406, *q*(F) –0.532, *q*(C) –0.058; and (b) θ 84.20°, *r*[C–F] 1.465 Å, *r*[Mg–C] 2.517 Å, *r*[Mg–F] 2.200 Å, *q*(Mg) 0.436, *q*(F) –0.222, *q*(C) 0.178.

listed in Table 3. They nicely fit those computed by the B3LYP method, as well as experimental obserables [10]. In place of ν(Mg–F) and ν(Mg–C), one frequency arises. It corresponds to vibrations of a system consisting of two bonds [ν(C–Mg–F)], symmetric (s) and antisymmetric (as), respectively. As would be expected, the formation of a strong C–Mg bond shifts C–H vibrations to lower frequencies compared to those observed for CH_3F (Table 2) and a number of Grignard complexes with a long Mg–C bond [Table 3 (θ 44.20 and 98.10°)].

Unlike curve S, curve T, the triplet component of the E_{tot}–θ function of the the Grignard complex displays a nonequilibrium process. Like with CH_3F, it slowly descends along the reaction coordinate (in our case, change in angle θ). However, in the course of the Grignard reaction curve T intersects curve S twice at bif1 67.80° and bif2 138.90°. At 68° < θ < 138°, curve T goes below curve S (Fig. 3). Beyond this range, curve T goes above curve S. The change in the total energy (curve T) in the range 150° < θ < 180° is insignificant and does not exceed 3–4 kcal/mol. The calculated frequencies and intensities of normal modes in the bif1 and bif2 points are given in Table 3. They occupy an intermediate position between the extreme points θ 44.20 and 180°.

Mechanism of Grignard reaction. Following the MERP principle [16], the reaction of Mg with CH_3F under normal conditions (no laser excitation of Mg, as in [10]) starts as a singlet process. Being highly exothermic, the reaction is slow from the very beginning [1, 12, 13] (its further acceration is due to the high exothermicity), facing an energy barrier (Fig. 3, curve S). However, as the reaction proceeds along curve S, the singlet and triplet states turn to be equal in energy and mix near bif1. With increasing θ, the triplet state becomes energetically preferable. This situation persists until bif2 is reached. According to the MERP principle, at the bif1 point switching from curve S to the nonequilibrium curve T occurs, after which the reaction proceeds along the latter curve.

Between the bifurcation points, the system Mg + CH_3F exists as a unified triplet ensemble (Figs. 4a, 4b). One can see spin density distribution between separate fragments of the Grignard complex at various θ angles. Figure 4a represents a three-dimensional map of spin density for θ 125.40° (*r*[C–F] 3.193 and *r*[Mg–C] 2.303 Å). The spin density embraces all the atoms, its major part being concentrated on the tightly bound fragment Mg–CH_3. To a first approximation, the latter can be regarded as purely triplet. The spin density on F is relatively autonomous. Therefore, at the given θ the fluorine atom can be considered to reside in the doublet state. As F is very distant from CH_3, the C–F bond is most likely hypothetical, so that F is held exclusively by the ionic-covalent Mg–F bond {*r*[Mg–F] 1.771 Å; *q*(Mg) 0.406 and *q*(F)

–0.532}. At θ 84.20° (Fig. 4b), there is another spin density distribution. In this case, the spin density embraces the Mg–F and Mg–CH_3 fragments, leaving the C–F bond (*r*[C–F] 1.465 Å) autonomous.

Similar reasoning regarding spin density distribution in the Grignard complex can be applied to other θ values. However, this is not necessary. As mentioned above, in the range bif1 < 0 < bif2 the Grignard complex is a unified triplet system. The considered doublet states are just limiting cases of a complex that is generally triplet in nature. That is why Walborsky's mechanism assuming occurrence of different radicals in the course of Grignard complex formation [5–7] (see above) is conceptually related to the idea of a superposition of a number of model structures like Kekule's benzene structures.

The triplet nature of the Grignard reaction (switching from curve S to curve T) is experimentally evidenced by the great number of reaction products [10] formed as a result of the uncompensated spin density on the C–F bond. Indeed, the effect of magnesium on the methyl group in the range 60° < 0 < 80° is insignificant because of the distance between them, while the Mg–F bond is practically leveled due to repulsion of negative charges (Table 3). For this reason, in the above θ range the CH_3–F fragment exists as an almost independent triplet molecule capable of spontaneous decomposition [Figs. 1, 3, nonequilibrium branch T; reactions (1)–(7)]. Particularly, this accounts for the formation of a broad spectrum of compounds (C_2H_6, CH_3Mg, $HMgCH_3$, CH_3MgCH_3, MgF, HF, and their various combinations [10]) in the Grignard reaction. The singlet reaction path (Davis's mechanism [9]; Fig. 3, curve S) cannot explain this observation.

The Grignard reaction is basically exothermic [1, 12, 13], which is supported by calculations (Fig. 3). The heat liberated in the reaction is sufficient to overcome the energy barrier at the bif1 and TS (curve S) points. Therefore, one should admit the possibility of both reaction paths: triplet–singlet and purely singlet (the triplet–singlet path is initiating). The two mechanisms differ substantially from one another. Switching to the triplet branch implies that Mg produces electron unpairing on the C–F bond, which immediately separates CH_3 and F, as shown above for the CH_3F molecule. However, in the case of the Grignard complex, these two fragments cannot become widely separated, because the positively charged magnesium ion tends to hold them together. Its insertion between the methyl group and fluorine to form a linear CH_3–Mg–F molecule appears to be quite natural. The methyl group and fluorine move away from each other. The magnesium, atom, tending to hold them together, approaches closer the line joining C and F. Geometrically, this means gradual increase of the H_3C–Mg–F angle. Unlike the above-considered case, the singlet process (curve S) is no more than pushing the CH_3 and F fragments away from each other by magnesium through changing charge and, consequently, distance parameters via electron density redistribution between the components of the complex. Hence, quite expectedly, the potential barrier for the singlet path of the reaction is 5.4 times higher than that for the triplet–singlet path (Fig. 3).

At the bif2 point, the energy levels of the triplet and singlet states, again, get closer to each other. Beyond this point, curve S goes below curve T (Fig. 3). In terms of the MERP principle, the Grignard reaction must be complete on curve S, ΔE_{tot}(T–S) 20.223 kcal/mol (θ 180°), which corresponds to formation of a stable form of the Grignard reagent. The exothermic nature of the Grignard reaction allows the T and S states to coexist after the bif2 point.

Conclusion. The performed calculations show that the Grignard reaction requires no external radiation. The triplet state of the Grignard complex emerges due to the presence of magnesium. Laser irradiation of magnesium surface [10] contributes only to acceleration of the process leading to the triplet state of Mg. The transition from the singlet state to triplet is underlied by spin-orbital electron interaction in the arising Grignard complex. In nonrelativistic quantum-chemical calculations, this interaction becomes appreciable if *d*,*p*-polarizing functions are included in the initial basis.

The Grignard reaction is just one model instance of mixing of singlet and triplet states, which demonstrates the diversified nature of processes involving magnesium. In fact, magnesium and its cationic forms play a crucial role in initiating many biological processes which, too, depend on the presence of singlet and triplet intermediates. Thus, self-assembly of tubulin and actin in living cells begins only in the presence of magnesium [22, 23]. Obviously, no external laser source is used in those natural processes. They occur in the dark, and the strongly delocalized triplet wave which gives rise to short-lived coherent biological ensembles [17–19, 24] emerges due to magnesium complexation with an appropriate amino acid environment.

Calculation methods. The calculations were carried out with CRAY YMP and CRAY STATION facilities at the Computer Center of California Technology Institute using the HF/UHF MP4(FULL)/6-311++G^{**} [25] method, GAUSSIAN-98 program

[26] and SO procedure [27]. The atomic charges were calculated with use of Lowdin's population analysis [28]. Physically, this method has advantages over Mulliken's one [29] which often leads to erroneous results [30]. Particularly, this explains the discrepancy between the charge, geometric, and other parameters of the Grignard reaction, obtained in the present work and reported earlier [9–11, 14].

ACKNOWLEDGMENTS

The author is grateful to Dr. V. Milligan for providing access to computer resources of California Technology Institute.

The author would like to dedicate the work to 100th anniversary of the discovery of the Grignard reaction (1900) and to its author Victor Grignard, a Nobel Prize winner (1912).

REFERENCES

1. Wakefield, B.J., *Organomagnesium Methods in Organic Synthesis. Best Synthetic Methods Series*, Katritzky, A.R., Meth-Cohn, O., and Rees, C.W., Eds., San Diego: Academic Press, 1995, p. 78.
2. Trofimenko, S., *Chem. Rev.*, 1993, vol. 93, no. 4, p. 943.
3. Bodineau, N., Mattalia, J.-M., Timokhin, V., Handoo, K., Negrel, J.-C., and Chanon, N., *Org. Lett.*, 2000, vol. 2, no. 3, p. 2303.
4. Wigal, C.T., *J. Org. Chem.*, 2000, vol. 62, no. 15, p. 4874.
5. Walborsky, H.M. and Young, A.E., *J. Am. Chem Soc.*, 1961, vol. 83, no. 16, p. 2595.
6. Walborsky, H.M. and Zimmermann, C., *J. Am. Chem. Soc.*, 1992, vol. 114, no. 22, p. 4996.
7. Hamdouchi, C., Topolski, M., Goedken, V., and Walborsky, H.M., *J. Org. Chem.*, 1993, vol. 58, no. 11, p. 3148.
8. Walter, R.L., *J. Org. Chem.*, 2000, vol. 65, no. 16, p. 5084.
9. Davis, S.R., *J. Am. Chem. Soc.*, 1991, vol. 113, no. 11, p. 4145.
10. Bare, W.D. and Andrews, L., *J. Am. Chem. Soc.*, 1998, vol. 120, no. 29, p. 7293.
11. Solov'ev, V.N., Sergeev, G.B., Nemukhin, A.V., Burt, S.K., and Topol, L.A., *J. Phys. Chem. A*, 1997, vol. 101, no. 46, p. 8625.
12. Grignard, V., *Compt. Rend.*, 1900, vol. 130, p. 1322.
13. Jones, P.R. and Southwick, E., *J. Chem. Educ.*, 1970, vol. 47, no. 3, p. 291.
14. Nemukhin, A.V., Topol, I.A., and Weinhold, F., *Inorg. Chem*, 1995, vol. 34, no. 11, p. 2980.
15. Pal'm, V.A., *Vvedenie v teoreticheskuyu organicheskuyu khimiyu* (Introduction to Theoretical Organic Chemistry), Moscow: Vysshaya Shkola, 1974.
16. Minkin, V.I., Simkin, B.Ya., and Minyaev, R.M., *Teoriya stroeniya molekul* (Theory of Molecular Structure), Rostov-on-Don: Feniks, 1997.
17. Buchachenko, A.L., *Usp. Khim.*, 1999, vol. 68, no. 2, p. 99.
18. Zewail, A.H., *J. Phys. Chem. A*, 2000, vol. 104, no. 24, p. 5660.
19. Zhong, D., Bernhardt, T., and Zewail, A.H., *J. Phys. Chem. A*, 1999, vol. 103, no. 49, p. 10093.
20. Becke, A.D., *J. Chem. Phys.*, 1993, vol. 92, no. 1, p. 1372.
21. Lee, C., Yang, W., and Parr, R.G., *Phys. Rev. B*, 1988, vol. 37, p. 785.
22. Tuszynski, J.A., Hameroff, S., Satarikc, M.V., Trpisova, B., and Nip, M.L.A., *J. Theor. Biol.*, 1995, vol. 174, no. 4, p. 371.
23. Weizenberg, R.C., Borisy, G.G., and Taylor, E.W., *Biochemistry*, 1968, vol. 7, no. 10, p. 4466.
24. Hutter, M.C., Hughes, J.M., Reimers, J.R., and Hush, N.S., *J. Phys. Chem. B*, 1999, vol. 103, no. 23, p. 4906.
25. Yuan, H. and Cremer, D., *J. Phys. Chem. A*, 2000, vol. 104, no. 32, p. 7679.
26. Frisch, M.J., Trucks, G.W., Schlegel, H.B., Scuceiria, G.E., Robb, M.A., Gheeseman, J.R., Zakrewski, V.G., Montgomery, J.A., Stratmann, R.E., Burant, J.C., Dapprich, S., Millam, J.M., Daniels, R.E., Kudin, K.N., Strain, M.C., Farhas, O., Tomasi, J., Barone, V., Cossi, M., Cammi, R., Menucci, B., Pomelli, C., Adamo, C., Clifford, S., Ochterski, J., Peterson, G.A., Ayala, P.Y., Cui, Q., Morokuma, K., Malick, D.K., Rabuck, A.D., Raghava-Chari, K., Foresman, J.B., Cioslowski, J., Ortiz, J.V., Stefanov, B.B., Liu, G., Liashenko, A., Piskorz, P., Komaromi, I., Gomperts, R., Martin, R.L., Fox, D.J., Keith, T., Al-Laham, M.A., Peng, C.Y., Nanayakkara, A., Gonzalez, C., Challacombe, M., Gill, P.M.W., Johnson, B., Chen, W., Wong, M.W., Andres, J.L., Gonzalez, C., Head-Gordon, M., and Pople, J.A., *GAUSSIAN 98*, Revs. A.5, A.7, Pittsburgh: Gaussian, 1998.
27. Vallet, V., Maron, L., Teichteil, C., and Flament, J.-P., *J. Chem. Phys.*, 2000, vol. 113, no. 4, p. 1391.
28. Mulliken, R.S., *J. Chem. Phys.*, 1955, vol. 23, no. 7, p. 1841.
29. Cioslowski, J. and Mixon, S., *J. Am. Chem. Soc.*, 1991, vol. 113, no. 11, p. 4142.
30. Lowdin, P.-O., *Adv. Quant. Chem.*, 1970, vol. 5, no. 1, p. 185.